Chapter 5

Development of Amorphous Silicon Alloy Thin Film Light Emitting Diode Having a-SiO:H as a Luminescent Layer

5.1 Introduction

It has been described in chapters 3 and 4 that visible-light amorphous thin film LEDs (TFLEDs) have been developed from the wide optical energy gap amorphous silicon alloys so-called a-SiN:H and a-SiC:H. The brightness obtained by these materials was the level of 1-2 cd/m^2. The advantages of these amorphous TFLEDs are for example, large area and low cost display and possibility of deposition on various kinds of substrates. However, a practical display requires higher brightness. Another candidate of amorphous silicon alloys that possesses wide optical energy gap and has capability to emit visible-light is hydrogenated amorphous silicon oxide (a-SiO:H).

Silicon oxide (SiO) and a-SiO:H materials have been generally used as insulating materials so far [1]. Other interesting applications of SiO and a-SiO:H have been expanding into electronic devices such as a gate layer in field effect transistor (FET) [2], a passivation layer and an anti-reflection layer in solar cell, etc.

It has been reported that a-SiO:H exhibits visible photoluminescence [3-5]. However, there has been no report on the application of the luminescent properties of a-SiO:H to any LED so far. Therefore, it is of great interesting to examine the possibility of the application of a-SiO:H to the luminescent i-layer in the amorphous TFLED.

In this work, the application of a-SiO:H to the luminescent i-layer in the amorphous TFLED has been attempted for the first time [6]. The structure of the device is glass/ITO/p-a-SiC:H/i-a-SiO:H/n-a-SiC:H/Al. In this chapter, a series of the technical data on the fabrication technology and basic characteristics of undoped a-SiO:H and results on the application to the i-layer in the TFLED are presented. It is

found that the brightness of the a-SiO:H TFLED is 0.3-0.5 cd/m^2. The result of the comparison of the brightness of the TFLEDs with different materials in the i-layers indicates that the TFLED with a-SiC:H as the i-layer gives the highest brightness. while the a-SiN:H shows the brightness higher than a-SiO:H. The data of ESR show that the spin density of a-SiO:H is higher than those of a-SiC:H and a-SiN:H. Although the a-SiO:H TFLED gives the lowest brightness, it is the first time to report that a-SiO:H can be applied as a luminescent layer in an amorphous visible-light TFLED.

5.2 Preparation of a-SiO:H Films

Hydrogenated amorphous silicon oxide (a-SiO:H) was prepared by the glow discharge plasma CVD system as mentioned in chapter 2. SiH_4 (diluted in H_2 to 10 %) and CO_2 (diluted with H_2 to 10%) were used as source gases. It was reported that CO_2 can provide oxygen and good quality of films [7-8]. The substrate temperature was 190 °C. The total gas pressure during the deposition was 1 torr. The typical preparation conditions for undoped a-SiO:H are summarized in Table 5.1. The deposition rate of undoped a-SiO:H was in the range between 0.27-0.51 Å.

Table 5.1 Typical preparation conditions for undoped a-SiO:H by the glow discharge plasma CVD method.

RF power	4 watt, 13.56 MHz
Substrate Temperature	190 °C
Gas Pressure	1 Torr
Gas Fraction	$x = CO_2/(SiH_4 + CO_2) = 0 \sim 0.7$

5.3 Structural Properties of a-SiO:H Films

Figure 5.1 shows IR absorption spectrum for undoped a-SiO:H prepared at the gas fraction $CO_2/(SiH_4+CO_2) = x = 0.35$. The main peaks arise from the absorptions of Si-H_2 (stretching) at 2090 1/cm, Si-O-Si (stretching) at about 1000 1/cm, Si-O-Si (bending) at 820 1/cm and Si-H (bending) at 640 1/cm. The absorption at 1000 1/cm

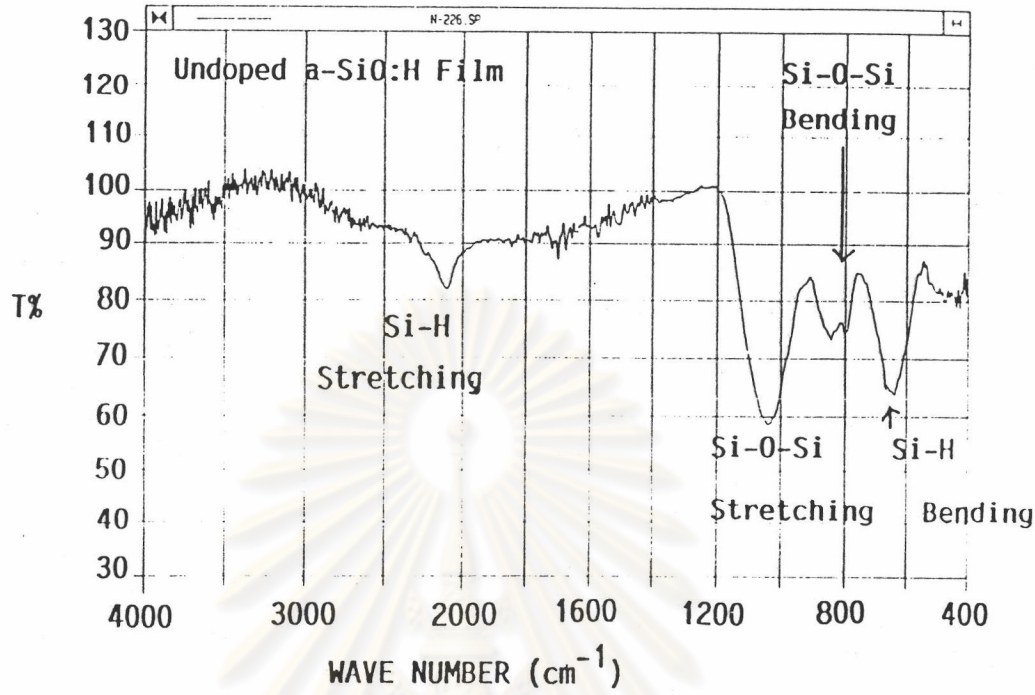

Figure 5.1 IR absorption spectrum for undoped a-SiO:H prepared at the gas fraction $CO_2/(SiH_4+CO_2) = x = 0.35$.

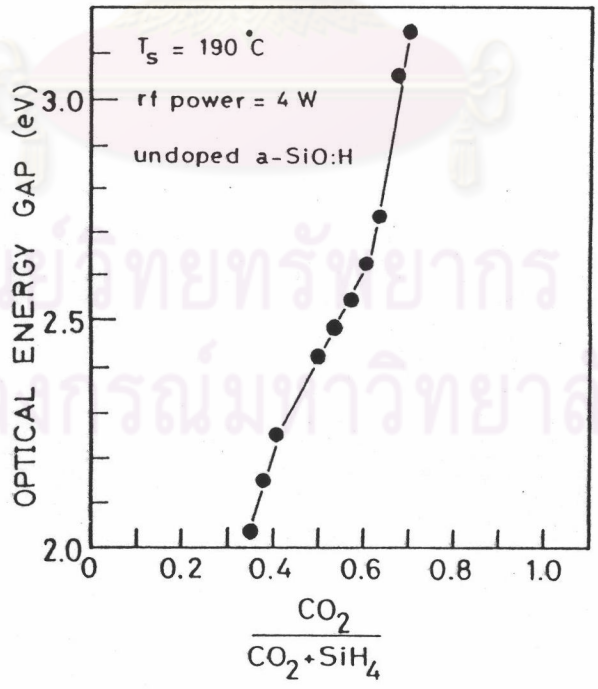

Figure 5.2 Relationship between the optical energy gap derived from Tauc's plot and the gas fraction $CO_2/(SiH_4+CO_2)$ for undoped a-SiO:H.

increases with increases in oxygen content while the vibration bond of O-H at 3600 1/cm was not observable. Therefore, the main bonding of oxygen atom is based on the form of Si-O-Si. The measurement of ESCA revealed that the carbon content was below the detection limit of the ESCA, i.e., 0.5%. The hydrogen and oxygen contents in these films were approximately 20-30 and 5-10 at.%, respectively.

The ESR spin density of the films were in the range of 10^{17}-10^{18} 1/cm^3. The spin density increases, with the CO_2 gas fraction increases [9].

5.4 Optical Properties of a-SiO:H Films

5.4.1 Optical Absorption Edge of a-SiO:H Films

Figure 5.2 shows the relationship between the optical energy gap derived from Tauc's plot and the gas fraction $CO_2/(SiH_4+CO_2)$ for undoped a-SiO:H. The optical energy gap of a-SiO:H increases monotonically from 1.7 eV to more than 3.2 eV with increasing the CO_2 gas fraction x from 0.35 to 0.70. As the CO_2 gas fraction increases, not only the optical energy gap shifts to higher energy but also the magnitude of the absorption coefficient at the energy region below the exponential tail drastically increases. The absorption spectra in this low energy region are generally considered to be due to the optical transitions from the defects states to empty states above the conduction edge.

5.4.2 Photoluminescence (PL) of a-SiO:H Films

Figure 5.3 shows PL spectra excited by 3250 Å HeCd laser of undoped a-SiO:H. The PL spectra show a single broad band. The emission color of the PL can be controlled from red (peak at 1.8 eV) to green (peak at 2.15 eV) by adjusting the optical energy gap from 2.25 eV to about 3.5 eV. The spectra shift toward higher energies with increasing the optical energy gap. At the same time the spectra tend to become broader, implying increased compositional fluctuation or an enhanced electron-phonon interaction.

Figure 5.4 summarizes the dependences of the PL peak energy and the optical energy gap for undoped a-SiO:H on the gas fraction x = $CO_2/(SiH_4+CO_2)$. The PL

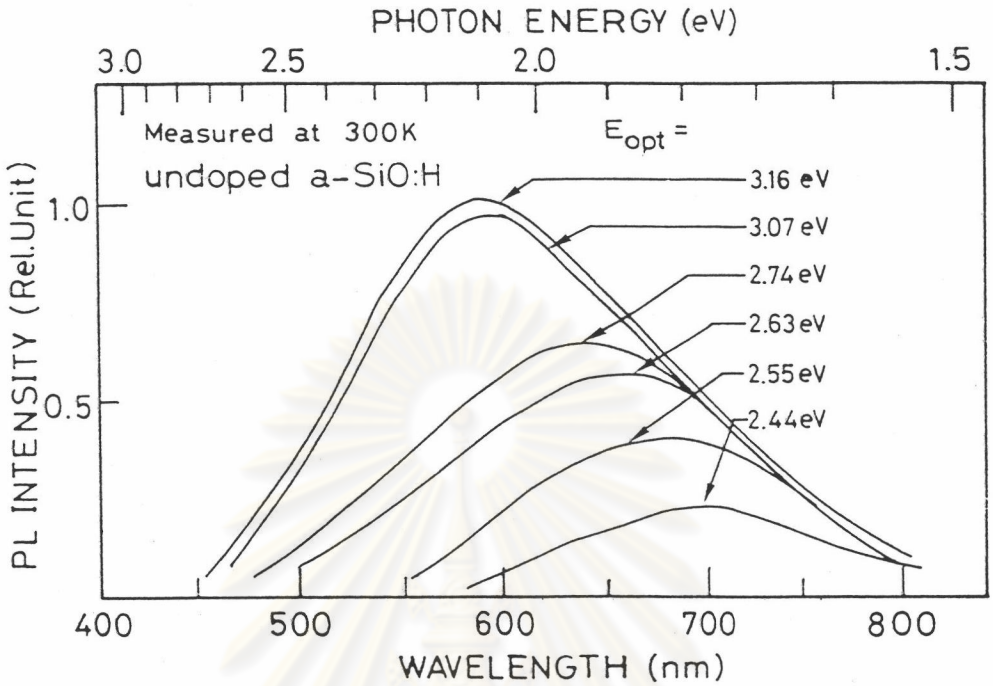

Figure 5.3 Room temperature PL spectra excited by 3250 Å HeCd laser of undoped a-SiO:H.

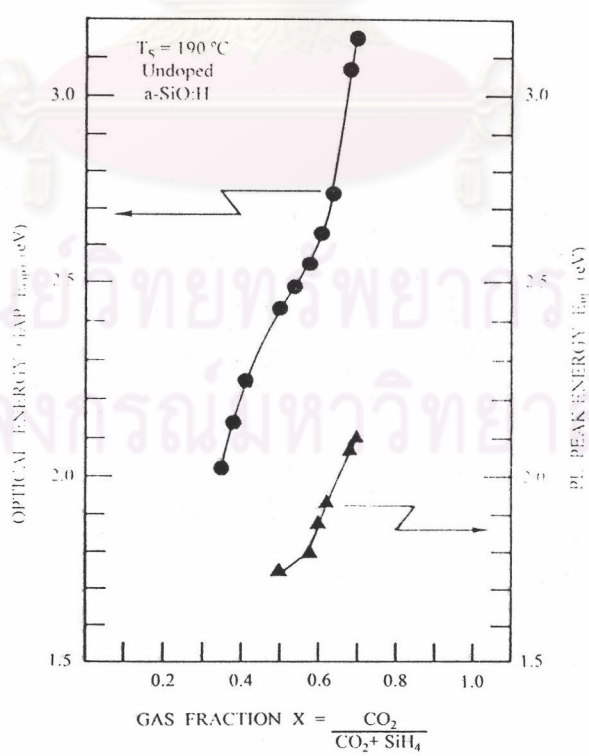

Figure 5.4 Dependences of the PL peak energy and the optical energy gap on the gas fraction $CO_2/(SiH_4+CO_2)$ for undoped a-SiO:H.

peak energy usually shows a stoke shift lying at an energy lower than its optical energy gap. The stokes shift might be caused by the distortion of lattices in part and/or by the relaxation of carriers down into deep states before recombinations take place. It is likely that as the optical gap increases, the value of E_{opt} - E_{PL} and the full width of PL spectrum become larger. This might imply that as the oxygen content increases, the distribution of the radiative recombination centers becomes broader and deeper within the gap.

5.5 Structure and Fabrication of Thin Film Light Emitting Diode Having a-SiO:H as a Luminescent Layer

a-SiO:H TFLED developed in this work has a structure of glass/ITO/ p-a-SiC:H/i-a-SiO:H/n a-SiC:H/Al [6]. Figure 5.5 shows a schematic illustration of the structure of an a-SiO:H TFLED. In this type of a-SiO:H TFLED, p- and n-layers act as injectors of holes and electrons, respectively, and the i-a-SiO:H acts as the luminescent layer. The thicknesses of p-i-n layers were 150, 500 and 500 Å, respectively, which were the same as used in the a-SiN:H and a-SiC:H TFLEDs. The optical energy gap of the luminescence i-layer for visible light was varied in the range 2.20 eV to 3.10 eV.

Figure 5.6 shows schematic band diagrams of an a-SiO:H TFLED in (a) thermal equilibrium and (b) forward bias conditions. The injection electroluminescence can be observed when the diode is a forwardly biased. In order to obtain a visible luminescence, the optical energy gap of the i-layer has to be larger than 2.3 eV, as deduced from the results of the photoluminescent data in the previous section. While the optical energy gaps of p- and n- a-SiC:H layers should be chosen around 2.0 eV to ensure the effective valency controllability to p- or n-type. Therefore, there exist the band discontinuities at the p/i and i/n interfaces as shown in Fig. 5.6.

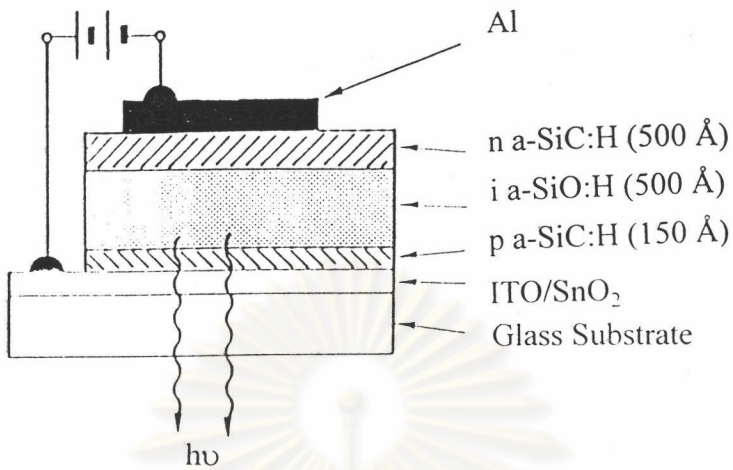

Figure 5.5 Schematic illustration of the structure of an a-SiO:H TFLED.

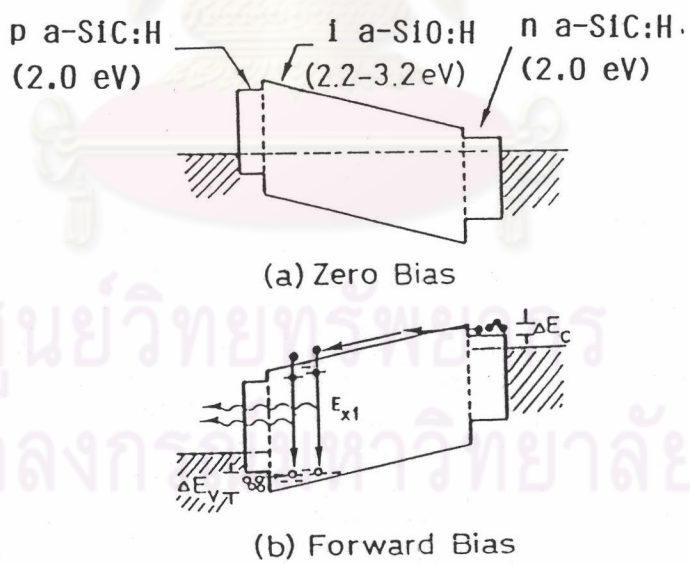

Figure 5.6 Schematic band diagrams of an a-SiO:H TFLED in (a) thermal equilibrium and (b) forward bias conditions.

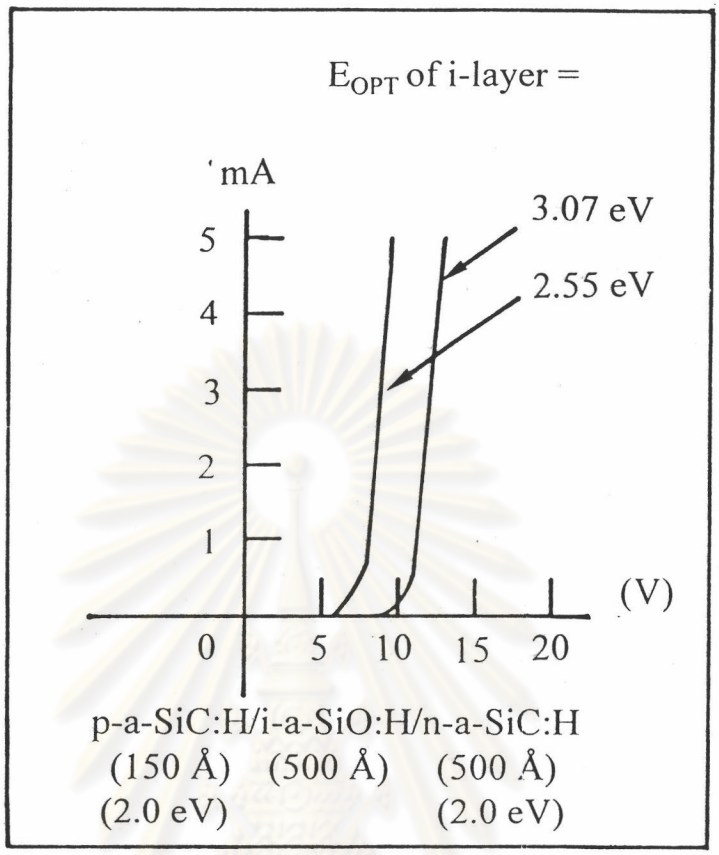

Figure 5.7 Room temperature I-V curves of an a-SiO:H TFLED. The parameter is the optical energy gaps of the i-a-SiO:H layer.

5.6 Basic Characteristics of a-SiO:H TFLED

In this section, basic characteristics including electrical properties and optical properties of the a-SiO:H TFLED are described.

5.6.1 Electrical Properties of a-SiO:H TFLED

Figure 5.7 shows I-V curves of an a-SiO:H TFLED measured at room temperature. The parameter is the optical energy gap of the i-a-SiO:H layer. The threshold voltages of these TFLEDs are in the range of 5 - 10 V. The emission was observed at the voltage above the threshold voltage.

5.6.2 Comparison of Brightness of a-SiN:H, a-SiC:H and a-SiO:H TFLEDs

The brightness of the emission from a-SiO:H TFLED is bright enough to be visually observed in a dim room. The brightness of a-SiO:H TFLED is about 0.30 cd/m^2.

It has been demonstrated in this work that the best structure of amorphous TFLEDs is based on the p-i-n junctions of the interesting amorphous silicon alloys. In this section, the brightnesses of TFLEDs prepared from different amorphous silicon alloys are compared.

Figure 5.8 (a) shows the structures of three types of amorphous TFLEDs fabricated in this work.

Sample # 1 has the structure of p-a-SiC:H/ i-a-SiC:H/ n-a-SiC:H.

Sample # 2 has the structure of p-a-SiC:H/ i-a-SiN:H/ n-a-SiC:H.

And sample # 3 has the structure of p-a-SiC:H/ i-a-SiO:H/ n-a-SiC:H.

The thicknesses of the p-i-n layers in all types of the TFLEDs were kept the same at 150 Å, 500 Å and 500Å, respectively. The optical energy gaps of the p-i-n layers for all types were kept the same at 2.0 eV, 3.0 eV and 2.0 eV, respectively.

It is found in Fig. 5.8 (b) that the brightness of the TFLED having a-SiC:H as the i-layer (sample #1) is better than those having a-SiN:H (sample #2) and a-SiO:H (sample #3) as the i-layers. One reason might be explained by a comparison of the defect densities of the films. The results from electron spin resonance (ESR) clarify

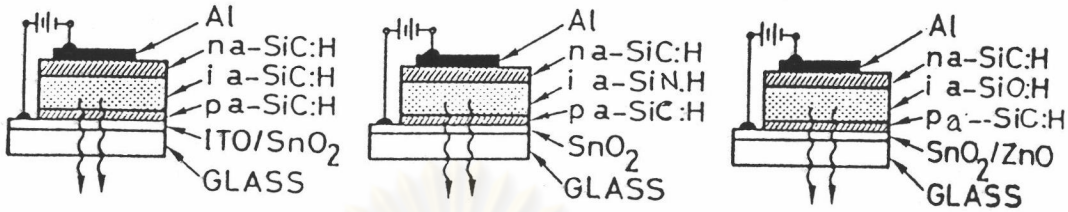

(Sample #1) (Sample #2) (Sample #3)

(a)

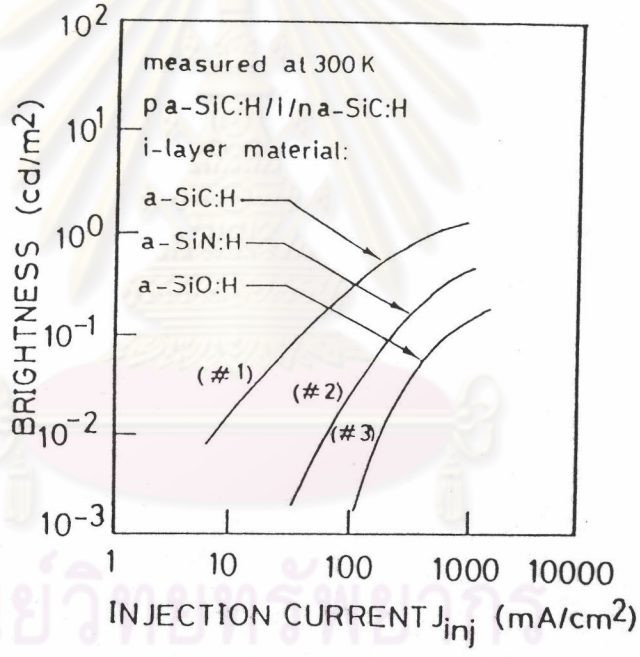

(b)

Figure 5.8 (a) Structures of three types of amorphous TFLEDs.
Sample # 1 has the structure of p-a-SiC:H/ i-a-SiC:H/ n-a-SiC:H.
Sample # 2 has the structure of p-a-SiC:H/ i-a-SiN:H/ n-a-SiC:H.
Sample # 3 has the structure of p-a-SiC:H/ i-a-SiO:H/ n-a-SiC:H.
(b) Comparisons of the brightness of amorphous TFLEDs. The parameter is the i-layers of the amorphous TFLEDs.

that the spin densities of a-SiO:H and a-SiN:H are higher than that of a-SiC:H. Although the brightness of the TFLED with a-SiO:H as the i-layer is not so good as those of the TFLEDs with a-SiC:H and a-SiN:H as the i-layers, it was confirmed in this work that undoped wide band gap a-SiO:H can be applied to the i-layer in the visible TFLED.

5.7 Summary

A novel visible-light amorphous p-i-n junction thin film LED (TFLED) having undoped a-SiO:H as the luminescent layer has been fabricated for the first time. The brightness of the a-SiO:H is approximately 0.3-0.5 cd/cm^2. This is the first trial that uses the semiconductor property of the a-SiO:H to the light emitting device. The undoped a-SiO:H was prepared from the mixture of SiH_4 and CO_2. A comparison has been done on the brightness of TFLEDs that the i-layers were prepared from three different materials, i.e., a-SiC:H, a-SiN:H and a-SiO:H. The result shows that the best brightness was obtained in the a-SiC:H, then less brightness in a-SiN:H and a-SiO:H, respectively.

In the next chapter, some efforts will be done for the purpose of the improvement of the brightness of amorphous TFLED. The effort will be concentrated on a-SiC:H TFLEDs.

References

1. Galeener, F.L. Current models for amorphous SiO_2. In Devine, R.A.B. (ed.) , The Physics and technology of amorphous SiO_2. pp. 1-15. Plenum press : New York and London, 1988.
2. LeComber, P.G. and Spear, W.E. The development of the a-Si:H field-effect transistor and its possible applications. In Pankove, J.I. (ed.) , Semiconductors and semimetals, Vol. 21 D. pp. 89-113. Academic press : New York, Tokyo. 1984.
3. Street, R.A. and Knights, J.C. Phil. Mag.B 42 (1980) : 551.
4. Carius, R., Fisher, R., Holzenkamfer, E., and Stuke, J. J. Appl. Phys. 52 (1981) : 4241.
5. Zacharias, M., Freisted, H., Stolze, F, Druseau, T.P., Rosenbauer, M., and Stutzmann, M. Properties of sputtered a-SiO_x:H alloys with a visible luminescence. J. Non-Crys. Solids 164-166 (1993) : 1089-1092.
6. Boonkosum, W., Kruangam, D., Ratvises, B., Sujaridchai, T., and Panyakeow, S. Visible amorphous SiO:H thin film light emitting diode. The 16th International Conference on Amorphous Semiconductors: Science and Technology (ICAS 16) Kobe. Japan. (September 4-8, 1995).
7. Fujikake, S., Ohta, H., Sichanugrist, P., Ohsawa, M., Ichikawa, Y., and Sakai, H. a-SiO:H films and their application to solar cells. Optoelectronic-Devices and Technologies. 9 (September 1994) : 379-390.
8. Sichanugrist, P., Sasaki, T., Asano, A., Ichikawa, Y., and Sakai, H. Amorphous silicon oxide and its application to metal/nip/ITO type a-Si solar cells. Technical Digest of the International PVSEC-7, Nagoya (1993) : 271-272.
9. Griscom, D.L. Intrinsic and extrinsic point defects in a-SiO_2. In Devine, R.A.B. (ed.) , The Physics and technology of amorphous SiO_2. pp. 125-134. Plenum press : New York and London, 1988.